

Pressure effects on the electronic properties and superconductivity in the pyrochlore oxides: AOs_2O_6 ($A = \text{Na}, \text{K}, \text{Rb}, \text{Cs}$)

R. Saniz and A. J. Freeman

Department of Physics and Astronomy, Northwestern University, Evanston, Illinois 60208-3112, USA
(dated: December 29, 2021)

We present a first-principles study of the electronic structure and superconducting parameters of the compounds AOs_2O_6 ($A = \text{Na}, \text{K}, \text{Rb}, \text{and Cs}$) and at ambient and applied hydrostatic pressure. We find that the sensitivity of the density of states at the Fermi energy, E_F , and related electronic properties to the size of the alkali metal atom as well as to applied pressure is driven by a van Hove singularity with energy very close to E_F . Further, a computation of the superconducting parameters of these materials allows us to show that the observed change of T_c , both upon substitution of the alkali metal and under applied hydrostatic pressure, can be well understood within a phonon-mediated pairing scenario. In this regard, we find that the correction to the effective electron mass due to spin fluctuations plays a significant role.

PACS numbers: 74.70.Dd, 71.20.Be, 74.25.Jb

I. INTRODUCTION

During the last decade or so, the search and interest in the superconductivity of non-Cu based oxides has extended from an effort to understand the pairing mechanism in the cuprates to a broader search of superconductivity in materials in which electron correlations are thought to play a determining role. To this end, researchers try to exploit a diverse range of factors, from the orbital degrees of freedom to the crystal structure of the material. A particularly interesting example is the recently discovered family of superconducting Os-oxide – pyrochlores AOs_2O_6 , with $A = \text{K}, \text{Rb}, \text{and Cs}$,^{1,2,3} which have superconducting transition temperatures $T_c = 9.6 \text{ K}, 6.3 \text{ K}, \text{ and } 3.3 \text{ K}$, respectively. The pyrochlore structure is a network of corner sharing tetrahedra and is a geometrically frustrated spin system if the ions bear a localized magnetic moment interacting antiferromagnetically with their nearest neighbors. Further, the Os ions located at the tetrahedra vertices possess a formal oxidation state of $5.5+$ ($5d^{2.5}$). As pointed out by Hiroi and co-workers,⁴ compared to other transition metal pyrochlore oxides, this places these materials between $\text{Cd}_2\text{Re}_2\text{O}_7$ ($\text{Re}^{5+} : 5d^2$), which is a good conductor at low temperatures^{5,6} (becoming superconductor at 1 K) and $\text{Cd}_2\text{Os}_2\text{O}_7$ ($\text{Os}^{5+} : 5d^3$), which is an insulator at low temperatures and exhibits antiferromagnetic ordering.⁷

While the several experimental results^{1,2,3,8,9,10,11,12,13} reported during the past year provide key information, the pairing mechanism in these materials is still under debate. These experiments indicate similarities but also differences among the compounds with different alkali metal, tending to single out KOs_2O_6 . Let us mention briefly some of the observations that should be taken into account by any proposed pairing mechanism. Firstly, the very change in T_c upon substitution of the alkali atom (A) may be initially counterintuitive. Indeed, the negative chemical pressure leads to an increase of the lattice con-

stant with the ionic radius of A , so that one may expect T_c to increase because band narrowing should lead to an increase of the density of states (DOS) at the Fermi level (E_F). As shown by the reported T_c 's above, however, the opposite occurs. In line with these findings, the change in T_c under applied hydrostatic pressure is found to be positive initially in all these materials.^{12,13} This has been interpreted as suggesting that the pairing mechanism in these materials is unconventional, or non-BCS-like.³ Of interest is the fact that in KOs_2O_6 the increase of T_c with pressure reaches a maximum at 0.56 GPa and tends to vanish gradually at higher pressures.^{13,14}

Further observations are that the temperature dependence of the resistivity shows an unusual concave behavior at low temperature in the case of KOs_2O_6 ,¹ while a T^2 behavior is observed² just above T_c in the case of RbOs_2O_6 and on a larger temperature interval³ in the case of CsOs_2O_6 . Also, nuclear magnetic resonance (NMR) experiments reveal a weak temperature dependence of the Knight shift of both the ^{39}K and ^{87}Rb nuclei in the corresponding pyrochlores.^{9,10} In the normal state, however, the relaxation rate divided by temperature ($1/T_1$) follows the Korringa relaxation in the case of Rb ,⁹ or deviates weakly from it,¹⁰ but deviates more strongly from this behavior in the case of K .¹⁰ In both cases, however, there appears to be evidence for antiferromagnetic spin fluctuations. Finally, regarding the superconducting gap, Magishi and co-workers find that the relaxation rate in the superconducting state suggests an anisotropic but nodeless gap⁹ in RbOs_2O_6 ; at the same time, Koda and collaborators interpret their muon spin rotation (SR) study of the magnetic penetration depth in KOs_2O_6 as pointing to an anisotropic gap with nodes.¹¹

We report here on a first-principles study of the electronic structure and superconducting parameters of the compounds AOs_2O_6 ($A = \text{Na}, \text{K}, \text{Rb}, \text{and Cs}$) and on the effects of hydrostatic pressure. We find that the main traits of the electronic structure reported previously¹⁵

TABLE I: Structural parameters of the OsO_6 -pyrochlores within the GGA approximation ($T = 0 \text{ K}$).

Compound	a (Å)	x	b_{OsO_6} (Å)	$\angle \text{O}-\text{Os}-\text{O}$	$\angle \text{OsO}_6-\text{OsO}_6$	B (GPa)
NaOsO_6	10.274	0.317	1.942	88.26	138.57	113.9
KOsO_6	10.298	0.316	1.944	88.54	138.98	116.6
RbOsO_6	10.318	0.315	1.945	88.82	139.39	118.8
CsOsO_6	10.356	0.314	1.948	89.27	140.03	123.8

in the case of KOsO_6 are common to all these materials, with relatively small qualitative and quantitative changes. The differences stem essentially from the energy level with respect to E_F of the van Hove singularity (vHS) with momentum k near the center of the Γ -L line. In particular, the density of states at the Fermi energy, $N(E_F)$, tends to increase with the size of A because the vHS is pushed closer to E_F . The effect of applied hydrostatic pressure is to push the vHS away from E_F . This is very clearly reflected by the increase or suppression of a constriction between the two Γ -point centered Fermi surface shells, basically due to a bending of the outer shell that depends on the proximity of the vHS to E_F .

We further estimate T_c with the well-known McMillan-A Allen-Dynes expression,¹⁶ with the electron-phonon coupling constant calculated within the crude rigid-muffin-tin approximation (RM-TA).^{17,18} We also calculate the Stoner susceptibility enhancement parameter and estimate the electron-spin coupling constant within the Doniach-Engelsberg approximation.¹⁹ This allows us to show that spin fluctuations contribute importantly to the effective electron mass, significantly reducing T_c . Despite the approximations implicit in these calculations, we find, remarkably, that the calculated T_c follows rather well the trends observed in experiment, both upon substitution of the alkali metal and under hydrostatic pressure. Our results, thus, bring further support to the electron-phonon coupling description of these superconductors.^{8,9,12,15}

Section II is devoted to the methodology of our calculations as well as to structural properties; in section III, we present and discuss our results in relation to the experimental findings mentioned above.

II. METHODOLOGY AND STRUCTURAL ASPECTS

We use the highly precise full-potential linearized augmented plane-wave (FLAPW)²⁰ implementation of the density functional approach to the electronic structure and properties of crystalline solids. We make our self-consistent calculations within the Perdew, Burke, and Ernzerhof generalized gradient approximation (GGA)²¹ to the exchange-correlation potential and include the spin-orbit coupling (SOC) term in the Hamiltonian. Angular momenta up to $l = 8$ are used for both the charge density in the muffin-tins and the wave functions. The irreducible part of the Brillouin zone is sampled with a uniform mesh of 120 k -points. The Os 5p and K 3p states

are treated as valence electrons.

The OsO_6 -pyrochlores crystallize in a cubic structure with space group $Fd\bar{3}m$. There are 18 atoms in the unit cell: two A atoms (8b), four Os atoms (16c), and twelve O atoms (48f). The Os atoms are octahedrally coordinated by six O atoms. An internal parameter, x , fixes the positions of the latter and thereby also determines the degree of rhombohedral distortion of the octahedra enclosing the Os atoms. In all the cases considered, we determine the lattice constant, a , as well as x , by minimizing the total energy and ensuring the total force on the O atoms is less than 10^{-4} a.u. The muffin-tin radii used are 2.2 a.u. for the Os ions and 1.3 a.u. for the O ions. The corresponding values for the Na, K, Rb, and Cs ions are, respectively, 2.6, 2.8, 3.0, and 3.1 a.u.

The values of the calculated structural parameters are reported in Table I, including the smaller $\text{O}-\text{Os}-\text{O}$ angle defining the main rectangular cross section of the octahedra and the $\text{O}-\text{Os}-\text{O}$ angle characterizing the staggered OsO_6 chains on the underlying the pyrochlore lattice. The calculated ($T = 0 \text{ K}$) lattice constants differ from the (room temperature) experimental results of Hiroi and co-workers (see Ref. 13) by +1.95% for KOsO_6 , +1.98% for RbOsO_6 , and +2.00% for CsOsO_6 . Although the compound with Na has not been synthesized, probably because of its small size, we have included it in our study to better identify the trends followed by the different properties upon A substitution. With respect to the other parameters in Table I, unfortunately the only experimental values reported are those of Bruhwyler et al.⁸ for RbOsO_6 . In this case, the difference of the calculated $\text{O}-\text{Os}$ bond length from experiment is +1.8%, while the difference for the internal parameter, and the $\text{O}-\text{Os}-\text{O}$ and $\text{OsO}_6-\text{OsO}_6$ angles are, notably, all below 0.1%. From Table I, it is clear that the angle in the OsO_6 chains increases with decreasing T_c . Assuming a phonon mediating pairing, it was suggested⁸ that this angle plays a role in determining T_c . Future studies of the phonon spectra of these materials should allow one to verify this interesting point. In Table I, we also give the calculated bulk moduli, which are necessary to calculate volume changes under pressure.

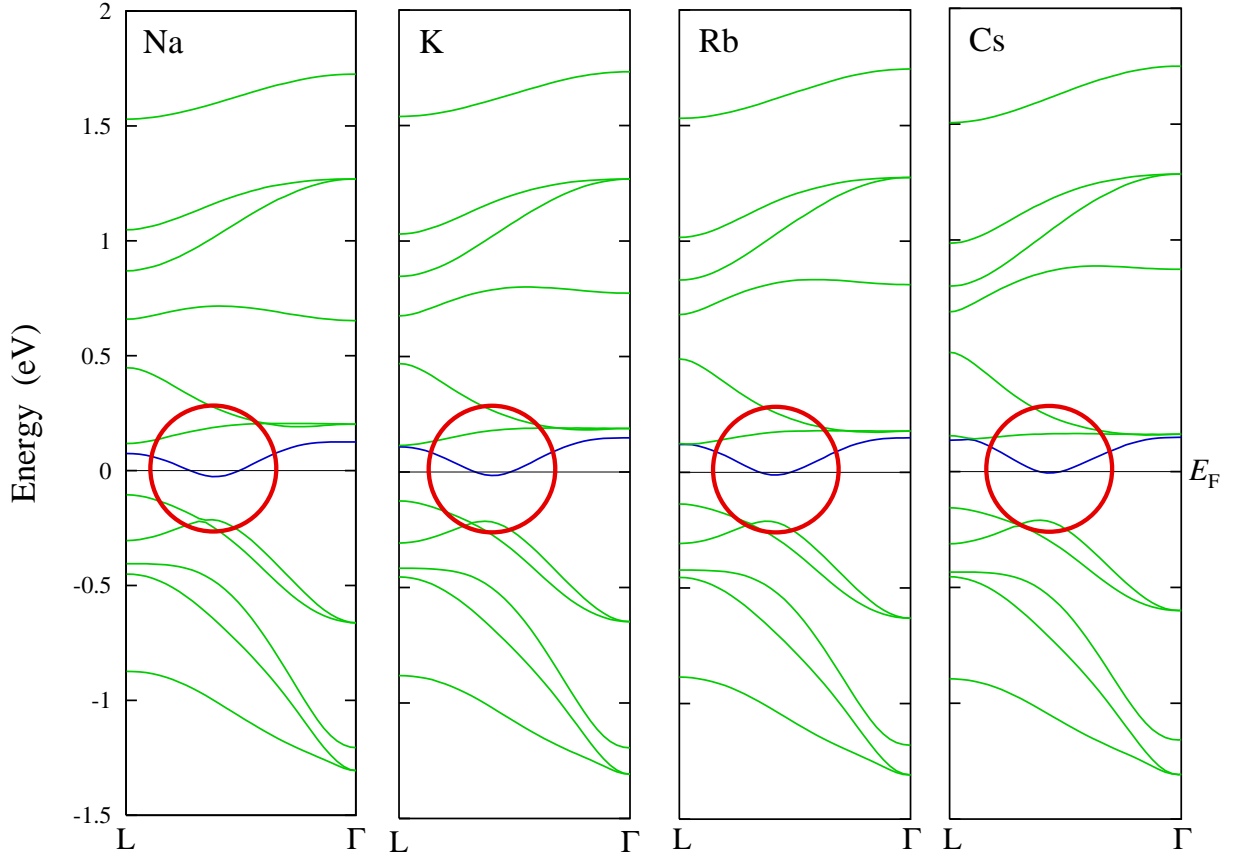


FIG. 1: (Color online) The manifold of 12 energy bands near E_F of the superconducting A -pyrochlore oxides plotted for k -points along the L - Γ line. The band crossing E_F is highlighted in blue, and the red circle indicates the location of the van Hove singularity. It is clearly seen that the larger the alkali metal, the closer the singularity is to E_F .

III. ELECTRONIC STRUCTURE AND PROPERTIES

A. Band structure and density of states

As we reported previously in the case of KOs_2O_6 ,¹⁵ we find that in all the A -pyrochlores the band structure around E_F is given by a manifold of twelve bands arising mainly from Os 5d states and O 2p states. The dispersion of the bands is generally the same for the different compounds, but there is an important difference near E_F , which is that the vHS near the center of the L - Γ line moves up closer to the Fermi level as the size of A increases. This is clearly illustrated in Fig. 1, where we compare the energy bands of the different compounds for k -points along the L - Γ . The consequence of this for DOS is also intriguing. Indeed, although the peak due to the vHS tends to decrease for the cases with a larger A ion, $N(E_F)$ increases because the vHS is closer to E_F . This is clear from Fig. 2, where we show a close-up of the total DOS around E_F for the different compounds. In Table II, where we list the total DOS at E_F , as well as the μ -spin sphere projected DOS for O and Os. For ref-

erence, we also indicate the values of the bare band Sommerfeld coefficient and of the band Pauli paramagnetic susceptibility. Comparing with measurements on powder samples, the specific heat mass-enhancements, $\gamma_{\text{exp}} = \gamma_b$, appear to be 3.3 for KOs_2O_6 ($\gamma_{\text{exp}} = 19 \text{ mJ/K}^2 \text{ mol Os}$)⁴ and 3.7 for $RbOs_2O_6$ ($\gamma_{\text{exp}} = 44 \text{ mJ/K}^2 \text{ mol Os}$).²² If the results reported by Muramatsu et al. are used for $RbOs_2O_6$ and $CsOs_2O_6$ (both with $\gamma = 20 \text{ mJ/K}^2 \text{ mol Os}$)¹³ one finds mass enhancements of 3.4 and 3.2, respectively. We note, however, that very recently Hiroi and co-workers reported²³ specific heat measurements on a single crystal sample of KOs_2O_6 , which, making an estimate similar to the powder sample case, yields a surprising $\gamma_{\text{exp}} = 64.8 \text{ mJ/K}^2 \text{ mol Os}$. This results in an unusually large $\gamma_{\text{exp}} = \gamma_b \approx 11.4$.²⁴

The effect of hydrostatic pressure is basically to push the eigenvalues around E_F downward. We illustrate this in the case of $RbOs_2O_6$ in Fig. 3, where we show a close look at the bands around E_F both for a sample under zero pressure and a sample under simulated pressure such that the change in the lattice constant is $\Delta a/a = 2\%$. While this corresponds to a relatively large pressure, it shows clearly the effect on the vHS, pushing it away from E_F .

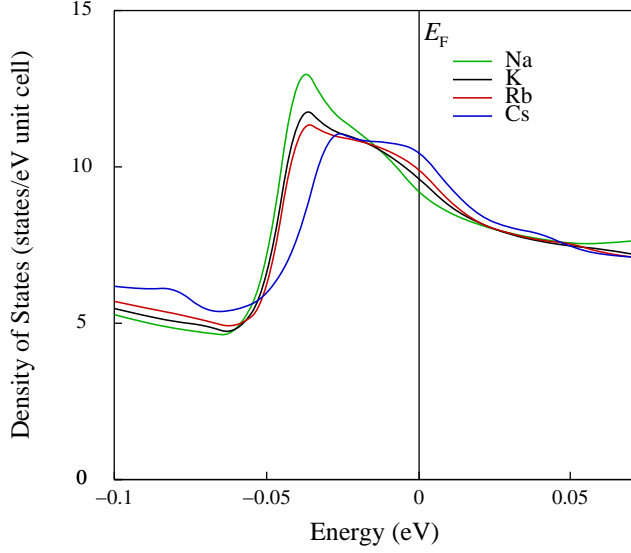


FIG. 2: (Color online) Density of states at E_F for the pyrochlore Os oxides. Although the height of the van Hove peak itself tends to decrease with the size the alkali ion, the value of $N(E_F)$ increases because the singularity shifts up in energy toward E_F .

TABLE II: Total DOS (states/eV unit cell) and mu n-tin sphere projected DOS (states/eV atom) at E_F . Also given are the bare band Sommerfeld coefficient ($\text{mJ/K}^2 \text{mol}_{\text{Os}}$) and the band Pauli paramagnetic susceptibility (10^6).

	NaOsO ₃	KOsO ₃	RbOsO ₃	CsOsO ₃
Total	9.13	9.64	9.96	10.58
A	0.019	0.020	0.030	0.048
Os	4.542	4.783	4.927	5.191
O	2.578	2.751	2.864	3.070
γ_b	10.76	11.36	11.74	12.46
χ_b	1.81	1.90	1.95	2.04

This naturally leads to a decrease of $N(E_F)$. As a further, quantitative illustration, in Table III we list $N(E_F)$ for various pressures in the case of $\text{KO s}_2\text{O}_6$.

As one may expect, the above effects are reflected in the topology of the Fermi surface. This is of general interest because of its direct relation to electronic properties and the possible effect of the vHS on quasi-particle lifetimes. The Fermi surface consists of two closed electron-

TABLE III: $N(E_F)$ as a function of pressure, for $\text{KO s}_2\text{O}_6$ (in states/eV unit cell).

V=V	P (GPa)	$N(E_F)$
0%	0	9.64
0.5%	0.583	9.47
1%	1.166	9.33
3%	3.498	7.24

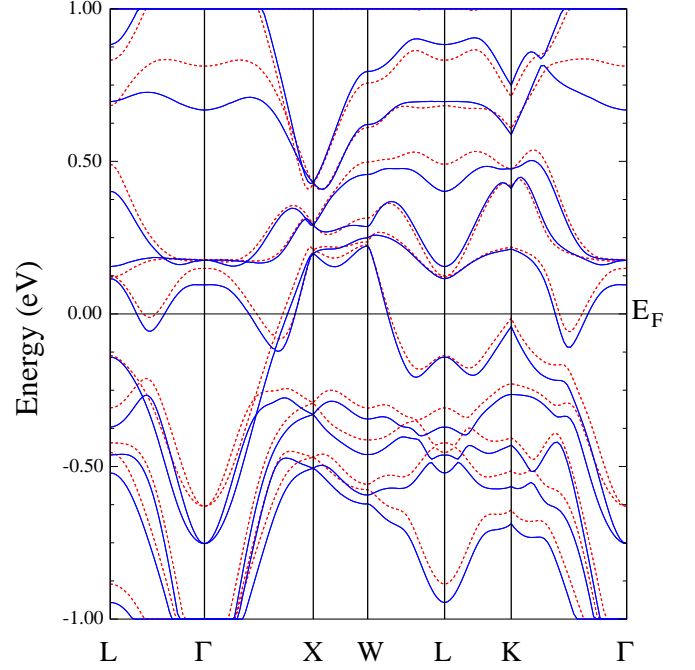


FIG. 3: (Color online) Band structure of RbOs_2O_6 for energies within 1 eV to E_F . Red-dotted curves: no pressure; solid-blue curves: hydrostatic pressure such that $a/a = 2\%$. Clearly, the the van Hove singularity is pushed away from E_F .

like sheets centered at the Γ point, and a third hole-like sheet giving rise to a tubular network. These Fermi surface sheets are shown in Fig. 4, plotted for clarity in the reciprocal unit cell. The tubular network actually does not present any major difference among the compounds considered; as a typical example we show the case of CsOs_2O_6 in Fig. 4(a). In contrast, the closed shells exhibit a clear difference near the midpoint of the $-\Gamma$ line, where the vHS is located. Indeed, in the case of NaOs_2O_6 , in Fig. 4(b), the two shells show no narrowing of the distance at this point, while the narrowing is obvious in the case of CsOs_2O_6 , as shown in Fig. 4(c). As discussed above, this is due to the closeness of the vHS to E_F in the latter case. The topology of the Fermi surface is also relevant to the superconducting gap. In relation to this, we note that the multi-band character of the Fermi surface and the different symmetry of its sheets may be of significance to some of the experimental results on the γ -pyrochlores. As pointed out above, Koda and co-workers interpret their results on the linear field dependence of the penetration depth, λ , as suggesting a non-conventional pairing mechanism in $\text{KO s}_2\text{O}_6$,¹¹ possibly mediated by magnetic fluctuations. However, in MgB_2 , which is a phonon-mediated superconductor, also exhibits such a linear dependence on the applied field.²⁵ In the case of MgB_2 this arises because of its

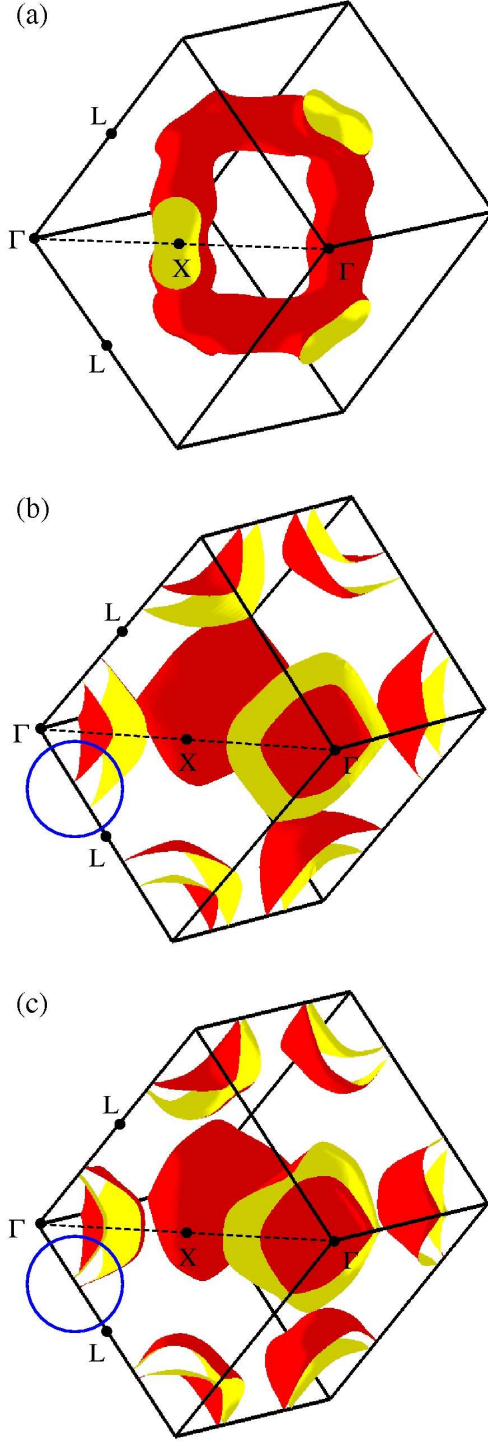


FIG. 4: (Color online) Fermi surface sheets of the π -pyrochlore O s oxides, plotted in the reciprocal unit cell. The "outer" surfaces of the sheets are colored red, while the "inner" ones are yellow. (a) The hole-like tubular network, which does not change noticeably under change of the alkali metal. (b) The closed shell surfaces around the X point for $\text{NaO s}_2\text{O}_6$. No constriction along the π -L line is seen (cf. circle). (c) The constriction near the center of the π -L line, indicated by the circle, in the case of $\text{CsO s}_2\text{O}_6$ is clear.

TABLE IV: Electron-phonon coupling parameters of the O s oxide π -pyrochlores in the RM TA approximation, with $\Theta_D = 285$ K. Hop eld parameters in $\text{eV}/\text{\AA}^2$.

Compound	Λ	α_s	α	λ_{ep}
$\text{NaO s}_2\text{O}_6$	$3 \cdot 10^{-6}$	0.421	0.126	0.84
$\text{KO s}_2\text{O}_6$	$1 \cdot 10^{-4}$	0.439	0.133	0.85
$\text{RbO s}_2\text{O}_6$	$2 \cdot 10^{-4}$	0.449	0.137	0.80
$\text{CsO s}_2\text{O}_6$	$5 \cdot 10^{-4}$	0.464	0.145	0.77

two-gap nature, which in turn is due to the particular character of its Fermi surface sheets, which we find akin to the present case to some extent.

B. Superconducting parameters

In the following, we examine the ability of a phonon-mediated pairing scenario to account for the experimental evidence, and, more particularly, the effects of alkali metal substitution and of pressure. To this end, we estimate the electron-phonon coupling constant λ_{ep} within the McMillan-Hop eld framework,^{26,27} and the crude rigid-mu n-tin approximation.^{17,18} The spherically averaged Hop eld parameter can be written²⁸

$$\lambda_{ep} = \frac{1}{N(E_F)} \sum_i \frac{M_{i,i+1}^2}{(2i+1)(2i+3)} \frac{N_{i_1}(E_F)N_{i_1+1}(E_F)}{N(E_F)}; \quad (1)$$

where $N_{i_1}(E_F)$ is the l-angular momentum DOS projected on the mu n-tin sphere of atom i ; $M_{i,i+1}^2 = \frac{1}{2} \frac{d}{dR_i} \left[\frac{1}{R_i} \left(\frac{d}{dR_i} \right)^2 \right] \left[\frac{1}{R_i} \left(\frac{d}{dR_i} \right)^2 \right] + (E_F - V_i) R_i^2$ is an electron-phonon matrix element, in terms of the logarithmic derivatives (D_{i_1}) and the partial wave amplitudes (ϕ_{i_1}) , both evaluated at E_F and at the mu n-tin radius (R_i) ; V_i is the one-electron potential at R_i . Then we have $\lambda_{ep} = \frac{1}{N(E_F)} \sum_i \frac{M_{i,i+1}^2}{(2i+1)(2i+3)}$, where M is the average mass.²⁹ As is common, the average phonon frequency is estimated in terms of the Debye temperature as $\hbar^2 \omega_D^2 = 0.69 \Theta_D^2$.

Regarding the Debye temperatures, there is unfortunately no experimental information for $\text{KO s}_2\text{O}_6$ and $\text{CsO s}_2\text{O}_6$. In the case of $\text{RbO s}_2\text{O}_6$, recent measurements suggest that the specific heat does not follow the usual

T^3 Debye model,³⁰ so that it is not clear what effective Θ_D is appropriate in our case. With this caveat, in our estimates we use the value $\Theta_D = 285$ K at $T = 6$ K obtained if a parametrization of the heat capacity in terms of a T dependent Θ_D is enforced.³⁰ In Table IV, we present our results for the λ_i and λ_{ep} for the different compounds.³¹

The critical temperature is subsequently calculated with the McMillan-A llen-D ynes equation^{16,32}

$$T_c = \frac{\hbar^2 \omega_D^2}{1.2} \exp \left[-\frac{1.04(1 + \lambda_{ep} + \lambda_{sp})}{\lambda_{ep} (1 + \lambda_{sp}) (1 + 0.62 \lambda_{ep})} \right]; \quad (2)$$

TABLE V : Superconducting parameters of the O s oxide pyrochlores. U is the Coulomb pseudopotential; I and S are the Stoner parameter and susceptibility enhancement factor, respectively, and J_{sp} is the electron-spin coupling constant; T_c^0 denotes the calculated critical temperature with $J_{sp} = 0$.

Compound		I (eV)	S	J_{sp}	T_c^0 (K)	T_c^{exp} (K)	T_c (K)
NaO S_2O_6	0.088	0.1166	2.14	0.054	10.9	—	7.0
KO S_2O_6	0.091	0.1166	2.28	0.064	11.0	9.6	6.4
RbO S_2O_6	0.093	0.1162	2.37	0.070	9.7	6.3	5.0
CSO S_2O_6	0.096	0.1155	2.57	0.084	8.8	3.3	3.6

where U is the Coulomb pseudopotential and J_{sp} is an effective electron-spin coupling constant. Note that, lacking the knowledge of the Eliashberg function $^2F(\omega)$, in lieu of the logarithmic average ω_{ln} we take the average phonon frequency, which we estimate in terms of ω_D , as indicated above.³³ The Coulomb pseudopotential can be estimated through $U = 0.26n(E_F) = [1 + n(E_F)]$, where $n(E_F)$ is the DOS at E_F per eV and atom.¹⁶ To estimate J_{sp} we use the expression derived by Doniach and Engelsberg $J_{sp} = 3IN(E_F) \ln[1 + 0.03IN(E_F)] = [IN(E_F)]^2$.^{19,34} The Stoner parameter in this expression, I , is calculated following the band formulation of Gunnarsson³⁵ and Brooks et al.³⁶ within spin-density-functional theory. More specifically, we have $I = \sum_i n_i I_i$; where n_i is the number of atoms of type i , and I_i the atomic Stoner parameter written as $I_i = \hat{n}_{i10} J_{i10}$. Here $\hat{n}_{i10} = N_{i1}(E_F)N_{i0}(E_F) = N_i^2(E_F)$ and $J_{i10} = \int d\mathbf{r} \int d\mathbf{r}' K(\mathbf{r}, \mathbf{r}') \psi_{i0}^2(\mathbf{r}) \psi_{i0}^2(\mathbf{r}')$ with, again, the partial wave amplitudes ψ_{i0} calculated at E_F . The exchange-correlation kernel K used is the one given by Gunnarsson.³⁵ In our case, the alkali atom contribution is completely negligible and only the diagonal $l=1$ term in O and the diagonal $l=2$ in S contribute because of the dominance of the respective partial DOS at E_F (see, e.g., Ref. 36). We note that our calculations are done taking spin-orbit coupling into account.

Our results for the superconducting parameters, as well as for I and the Stoner enhancement factor $S = [1 + IN(E_F)]^2$, are given in Table V. We note first that our calculated T_c (last column) follows well the experimental trend, although the range of the experimental T_c 's is noticeably larger. Clearly, however, a more refined calculation of J_{sp} based on, e.g., the frequency dependence of the Eliashberg function 2F , can easily account for the difference of a fraction to a few K between our results and experiment seen in Table V. In this regard, Kunes and co-workers³⁷ have found that the alkalis in these materials possess a varying degree of anharmonicity in the potential, which would add to the difference in their T_c 's. Secondly, we note the significant role of spin fluctuations. Indeed, with $J_{sp} = 0$ the predicted T_c (given as T_c^0) is 72% (KO S_2O_6) to 144% (CSO S_2O_6) higher. Thus, although the calculated Stoner enhancement factors ($2 < S < 3$) indicate that these systems are not close to a ferromagnetic instability, they are sufficient to produce a significant electron-spin coupling.

Finally, we have calculated the superconducting pa-

rameters of KO S_2O_6 (again with $\omega_D = 285$ K) under the simulated effect of pressure, to study the initial change of T_c with pressure. We have considered pressures up to 1.166 GPa, which is of the order of the pressures used in the experimental report by Muramatsu et al.¹³ Our results are given in Table VI. As in experiment,^{12,13} we see that T_c increases with pressure, although J_{sp} decreases. The main reason is that both U and J_{sp} also decrease, and more importantly the latter than the former. Hence, the initial increase of T_c with pressure appears to be due mainly to a decrease of spin fluctuations, driven by the decrease of $N(E_F)$ (the Stoner parameter I is almost unchanged). Comparing our results with the ratio $T_c = T_c^0 = 1.04$ found at 0.56 GPa by Muramatsu and collaborators,¹³ we see that the change in T_c is of the same order and is essentially accounted for. Indeed, if the main cause were to be phononic, i.e., a change in ω_D , the latter would have to decrease with pressure, contrary to any likelihood.³⁸ Again, we surmise that a more refined calculation can readily account for the somewhat steeper initial increase of T_c observed. In their experimental study of the change of T_c with pressure in the case of RbO S_2O_6 , Khasanov and co-workers had already concluded that the observed positive slope at low pressures must arise mainly from electronic contributions, as opposed to phononic ones, although the mechanism behind the effect was still an open question.¹²

We note that the very recent report by Muramatsu and collaborators³⁹ shows that in the present family of superconductors, after reaching a maximum value, with increasing pressure T_c will gradually decrease, falling below its ambient pressure value, until superconductivity is eventually suppressed. To make predictions of T_c at those high pressures, however, it would be necessary to have a minimum information on the phonon spectra and how they are affected by pressure. We do not know what would be a sensible value of ω_D to make such estimates of T_c within our approach. However, we can try to understand what happens as follows. If the Grüneisen parameter for KO S_2O_6 is around 1.8, which is a rough average for most substances,⁴⁰ then for a pressure $P = 3.5$ GPa (corresponding to $V = V' - 3\%$), $\omega_D = 301$ K. The calculated superconducting parameters ($U = 0.085$, $J_{sp} = 0.048$, and $J_{ep} = 0.738$) then would lead to $T_c = T_c^0 = 0.88$ (against 0.66 in experiment). This result suggests that the decrease of T_c at higher pressures could be understood as reflecting the

TABLE VI: Superconducting parameters as a function of pressure for KOs_2O_6 ($T_D = 285$ K). T_c^0 corresponds to 0 pressure.

Pressure (GPa)	S	sp	ep	$T_c = T_c^0$
0	0.091	2.28	0.064	0.852
0.583	0.090	2.23	0.060	0.845
1.166	0.089	2.19	0.057	0.841

fact that in that regime the phononic properties become dominant.

It is remarkable, given the approximate nature of our estimate of ϵ_p and T_c , that our results account rather well for the behavior of T_c under substitution of the alkali metal and under applied pressure. We believe this brings strong support for the phonon-mediated pairing scenario. To understand more fully the properties of the pyrochlore Os oxides, however, further investigation will be required, experimentally and theoretically. For instance, the different nuclear spin-lattice relaxation rates of the alkali ions in KOs_2O_6 and RbOs_2O_6 remain to be clarified. This could be partly due to the rapid variation of the DOS close to E_F . Indeed, Fig. 2 shows that $N(E_F)$ can change by as much as 50% within an energy range of 25 meV (more so the heavier the alkali ion). A further contribution may come from the changing character of the alkali atom DOS at E_F . We find that its character falls from 73% in NaOs_2O_6 , to 11% in CsOs_2O_6 , passing by 31% in KO_2O_6 and 23% in RbOs_2O_6 (at the

same time its p character rises from 16% in NaOs_2O_6 , to 55% in CsOs_2O_6 , passing by 31% in KO_2O_6 and 38% in RbOs_2O_6).

Furthermore, the origin of the unusual behavior of the resistivity in KOs_2O_6 at low T is also not understood, nor is the rather large specific heat mass enhancements $\epsilon_{\text{exp}} = b$ in all these materials. The electron-phonon and electron-spin coupling constants obtained above are clearly insufficient to account for the observed enhancements of 3(4). It is possible that the vHS near E_F and the nesting exhibited by the Fermi surface⁴¹ contribute to both the resistivity and the specific heat. The observed enhancements suggest, in our view, that the unusual non-Debye behavior at low temperature of the specific heat mentioned above is a generic property.

Acknowledgments

We thank Lin-Hui Ye, S. H. Rhim, J. B. Ketterson, and W. H. Halperin for helpful discussions. We are also grateful to B. Barbiellini and G. G. Rimmvall for their suggestions and to B. Batlogg and M. B. Hühner for sharing data with us prior to publication. This work was supported by the Department of Energy (under grant No. DE-FG 02-88ER 45372/A 021 and a computer time grant at the National Energy Research Scientific Computing Center).

- ¹ S. Yonezawa, Y. Muraoka, Y. Matsushita, and Z. Hiroi, J. Phys.: Condens. Matter 16, L9 (2004).
- ² S. Yonezawa, Y. Muraoka, Y. Matsushita, and Z. Hiroi, J. Phys. Soc. Jpn. 73, 819 (2004).
- ³ S. Yonezawa, Y. Muraoka, Z. Hiroi, J. Phys. Soc. Jpn. 73, 1655 (2004).
- ⁴ Z. Hiroi, S. Yonezawa, and Y. Muraoka, J. Phys. Soc. Jpn. 73, 1651 (2004).
- ⁵ M. Hanawa, Y. Muraoka, T. Tayama, T. Sakakibara, J. Yamamura, and Z. Hiroi, Phys. Rev. Lett. 87, 187001 (2001).
- ⁶ R. Jin, J. He, S. McCall, C. S. Alexander, F. Dymot, and D. Mandrus, Phys. Rev. B 64, 180503(R) (2001).
- ⁷ D. Mandrus, J. R. Thompson, R. Gaal, L. Forro, J. C. Bryan, B. C. Chakoumakos, L. M. Woods, B. C. Sales, R. S. Fishman, and V. Keppens, Phys. Rev. B 63, 195104 (2001).
- ⁸ M. B. Hühner, S. M. Kazakov, N. D. Zhigadlo, J. Karpinski, and B. Batlogg, Phys. Rev. B 70, 020503(R) (2004).
- ⁹ K. Magishi, J. L. Gavilano, B. Pedrini, J. Hinderer, M. Weller, H. Rott, S. M. Kazakov, and J. Karpinski, Phys. Rev. B 71, 024524 (2005).
- ¹⁰ K. Arai, J. Kikuchi, K. Kodama, M. Takigawa, S. Yonezawa, Y. Muraoka, and Z. Hiroi, cond-mat/0411460.
- ¹¹ A. Koda, W. Higemoto, K. Ohishi, S. R. Saha, and R. Kadono, cond-mat/0402400.
- ¹² R. Khasanov, D. G. Eshchenko, J. Karpinski, S. M. Kazakov, N. D. Zhigadlo, R. Bartsch, D. G. Avillet, D. D. Castro, A. Shengelaya, F. La Mattina, A. Maisuradze, C. Baines, and H. Keller, Phys. Rev. Lett. 93, 157004 (2004).
- ¹³ T. Muramatsu, S. Yonezawa, Y. Muraoka, and Z. Hiroi, J. Phys. Soc. Jpn. 73, 2912 (2004).
- ¹⁴ After the submission of this manuscript, Muramatsu and co-workers reported new high pressure measurements (pressures up to 10 GPa), showing that T_c follows a similar trend in all three compounds with $A = \text{K}, \text{Rb},$ and Cs , and that under appropriate normalization the plots of T_c vs. P appear to fall under a same universal curve. See Ref. 39.
- ¹⁵ R. Saniz, J. E. Medvedeva, Lin-Hui Ye, T. Shishidlov, and A. J. Freeman, Phys. Rev. B 70, 100505(R) (2004).
- ¹⁶ K. Bennemann and J. Garland, in Superconductivity in d- and f-band metals, edited by D. H. Douglass, AIP Conf. Proc. No. 4, (AIP, New York, 1972), p. 103.
- ¹⁷ G. P. Gasparyan and B. L. Gyorffy, Phys. Rev. Lett. 28, 801 (1972).
- ¹⁸ D. G. Pettifor, J. Phys. F: Metal Phys. 7, 1009 (1977).
- ¹⁹ S. Doniach and S. Engelsberg, Phys. Rev. Lett. 17, 750 (1966).
- ²⁰ E. Wimmer, H. Kalkauer, M. Weinert, and A. J. Freeman, Phys. Rev. B 24, 864 (1981); M. Weinert, E. Wimmer, and A. J. Freeman, ibid. 26, 4571 (1982); H. J. F. Jansen and A. J. Freeman, ibid. 30, 561 (1984).
- ²¹ J. P. Perdew, K. Burke, and M. Ernzerhof, Phys. Rev. Lett. 77, 3865 (1996).
- ²² M. B. Hühner, S. M. Kazakov, J. Karpinski and B. Batlogg,

- cond-m at/0502125.
- ²³ Z. Hiroi, S. Yonezawa, J.-I. Yamaura, T. Muramatsu, and Y. Muraoka, cond-m at/0502043.
- ²⁴ This result calls for similar measurements on the other Os oxide pyrochlores, not least because, in addition, a second peak is observed in the $C=T$ curve, below the superconducting T_c , which could indicate a further first-order or -type phase transition.
- ²⁵ K. Ohishi, T. Muranaka, J. Akimitsu, A. Koda, W. Higemoto, and R. Kadono, J. Phys. Soc. Jpn. 72, 29 (2003).
- ²⁶ W. L. McMillan, Phys. Rev. 167, 331 (1968).
- ²⁷ J. J. Hopfeld, Phys. Rev. 186, 443 (1969).
- ²⁸ H. L. Skriver and I. Mertig, Phys. Rev. B 32, 4431 (1985).
- ²⁹ There are several formulas to calculate ϵ_p in the case of compounds [see M.-C. Huang, H. J. F. Jansen, and A. J. Freeman, Phys. Rev. B 37, 3489 (1988), and references therein]. In our case, we think it is more sensible to take the average mass M instead of the atomic masses M_i , because it is known that the latter overweights the contribution of light atoms like O.
- ³⁰ M. Bruhwyler and B. Batlogg (private communication).
- ³¹ An estimate of a zero temperature ϵ_D from the elastic constants of these materials shows that it decreases with increasing size of A, and one can expect ϵ_D to follow the same trend. However, it is known that ϵ_D generally decreases quadratically with temperature at low temperatures (see, e.g., G. Grimvall, Thermophysical properties of materials (Elsevier, Amsterdam, 1999), p. 97), so that the observed decrease of T_c with the size of A is expected to result in ϵ_D at T_c moving upward, tending to compensate the first effect. Thus, we use the same ϵ_D for all the compounds in our calculations.
- ³² P. B. Allen and R. C. Dynes, Phys. Rev. B 12, 905 (1975).
- ³³ It is difficult to know beforehand whether the correction of $|\ln \overline{h}|^2 i^{1-2}$ is small or not for a given compound. However, the account presented here of the trends observed in experiment allows us a posteriori to expect that the correction will not be too large and that the physical content of our description will be preserved.
- ³⁴ As Doniach and Engelsberg (Ref. 19), we use a momentum cutoff $p=p_F = 0.6$.
- ³⁵ O. Gunnarsson, J. Phys. F: Metal Phys. 6, 587 (1976).
- ³⁶ M. S. S. Brooks, O. Erickson, and B. Johansson, Phys. Scr. 35, 52 (1987).
- ³⁷ J. Kunes, T. Jeong, and W. E. Pickett, Phys. Rev. B 70, 174510 (2004).
- ³⁸ As noted above (cf. Ref. 31), ϵ_D increases with decreasing lattice constant (positive chemical pressure), thus indicating a positive Grueneisen constant.
- ³⁹ T. Muramatsu, N. Takeshita, C. Terakura, H. Takagi, Y. Tokura, S. Yonezawa, Y. Muraoka, and Z. Hiroi, cond-m at/0502490.
- ⁴⁰ J. A. G. Schneider, Jr., in Solid State Physics Vol. 64, edited by F. Seitz and D. Turnbull (Academic Press, New York, 1964), p. 275.
- ⁴¹ In Ref. 37, a calculation of the bare band susceptibility along the $-K$ direction is reported for KOs_2O_6 . Although it appears not to suggest electronic instabilities, it does show clear nesting effects. We note that the constriction between the two closed Fermi surfaces discussed above may have effects on the nesting; in particular, it may degrade any nesting along the $[111]$ direction in the case of the heavier alkaline metals.